

Evaluation of a High Performance, Fixed-Ratio, Traction Drive*

Stuart H. Loewenthal,† Neil E. Anderson,‡ and Douglas A. Rohn†

Although light-duty, variable-ratio traction drives have been reasonably successful from a commercial standpoint (ref. 1), very few, if any, fixed-ratio types have progressed past the prototype stage. This is somewhat surprising in view of the outstanding ability of traction drives to provide smooth, quiet power transfer at extremely high speeds with good efficiency. They seem particularly well suited for high speed machine tools, pump drives, and other turbomachinery. However, the fixed-ratio traction drives of the past have generally not been weight or size competitive with their gear drive counterparts. There are several reasons for this. First, the steels used in earlier traction drives had significantly less fatigue life than today's metallurgically cleaner bearing steels. Second, the earlier traction drives did not benefit from the use of modern traction fluids, which can produce up to 50 percent more traction than conventional mineral oils for the same normal load (ref. 2). In addition, recent advancements in the prediction of traction-drive performance (refs. 3 to 6) and fatigue life (refs. 7 and 8), have added a greater degree of reliability to the design of these devices.

Perhaps the most significant reason why traction drives have not been competitive in size with gear systems is fundamental to the way they transmit torque. Unlike a simple gear mesh, the normal load imposed on a traction contact must be at least an order of magnitude larger than the transmitted traction force to prevent slip. Thus, to achieve high power density, the traction drive must be constructed with multiple, load-sharing roller elements to reduce the contact unit loading. This was recognized by Lubomyr Hewko who performed some of the earliest traction contact experiments (refs. 9 and 10). His data provided design information for a high performance, multicontact, simple planetary roller drive (ref. 11). The planetary arrangement ensured that the relatively large normal contact loads on the rollers were internally balanced and reacted by the ring-roller rather than by bearings. Tests with a 3.5 to 1 ratio, six planet, 75-kW unit (ref. 11) showed it to have better efficiency and substantially lower noise than a comparable planetary gearset. Recently, tests of a planetary type traction drive of similar construction for use with a gas-turbine APU system were reported in (ref. 12).

For traction drives with a simple, single-row planet-roller format, the number of load sharing planets is inversely related to the speed ratio. For example, a four-planet drive would have a maximum speed ratio of 6.8 before the planets interfered. A five-planet drive would be limited to a ratio of 4.8, and so on.

A remedy to the speed ratio and planet number limitations of simple, single-row planetary systems was devised by A.L. Nasvytis (ref. 13). His drive system used the sun and ring roller of the simple planetary traction drive, but replaced the single row of equal diameter planet rollers with two or more rows of stepped or dual-diameter planets. With this new multiroller arrangement, practical speed ratios of 150 to 1 could be obtained in a single stage with three planet rows. Furthermore, the number of planets carrying the load in parallel could be greatly increased for a given ratio. This resulted in a significant reduction in individual roller contact loading with a corresponding improvement in torque capacity and fatigue life.

Based on the inherent qualities of the Nasvytis configuration and the results from earlier prototype tests (ref. 13), a test program was initiated to evaluate the key operational and performance factors associated with the Nasvytis multiroller traction-drive concept. To accomplish this objective, two sets of Nasvytis drives, each of slightly different geometry, were parametrically tested on a back-to-back test stand. Initial results from these tests are reported in (ref. 14). One of these units was later retrofitted to the power turbine of an automotive gas-turbine engine and dynamometer tested.

*Previously published as NASA TM 81425; AVRADCOM 80-C-1.

†NASA Lewis Research Center.

‡Propulsion Laboratory, U.S. Army Research and Technology Laboratories (AVRADCOM), NASA Lewis Research Center.

Nasvytis Traction Drive Concept

The basic geometry of the Nasvytis traction drive is shown in figure 1. Two rows of five stepped planet rollers are contained between the concentric, high-speed sun and low-speed ring rollers. The planet rollers do not orbit but are grounded to the base through reaction bearings contained only in the second or outer row of planets. This is a favorable position for the reaction bearings since the reaction forces and operating speeds are relatively low.

The sun roller and the first row of planets float freely, relying on contact with adjacent rollers for location. Because of this self-supporting roller approach, the number of total drive bearings is greatly reduced, and the need for the often troublesome, high-speed shaft-support bearings has been eliminated. In addition, both rows of planets are in three-point contact with adjacent rollers, promoting a nearly ideal internal force balance. In the event of an unbalance in roller loading, the first and second row of planets (supported by large clearance bearings) will shift under load until the force balance is reestablished. Consequently, slight mismatches in roller dimensions, housing distortions under load, or thermal distortions merely cause a slight change in roller orientation without affecting performance. Because of this roller-cluster flexibility, the manufacturing tolerances set for dimensions can be rather generous relative to the standard set for mass-produced bearing rollers.

The number of planet-roller rows, the number of planet rollers in each row, and the relative diameter ratios at each contact are variables to be optimized according to the overall speed ratio and the uniformity of contact forces. In general, drives with two-planet rows are suitable for speed ratios to about 45, and drives with three-planet rows are suitable for ratios to about 250.

Geometry of Test Drives

Two sets of Nasvytis drives of nominally 14.7 to 1 and 14 to 1 ratios were tested. Both drive designs had two rows of five-planet rollers, each, but were equipped with different roller-cluster loading mechanisms. Figure 2 shows a cross section cut through the roller contact points of the drive

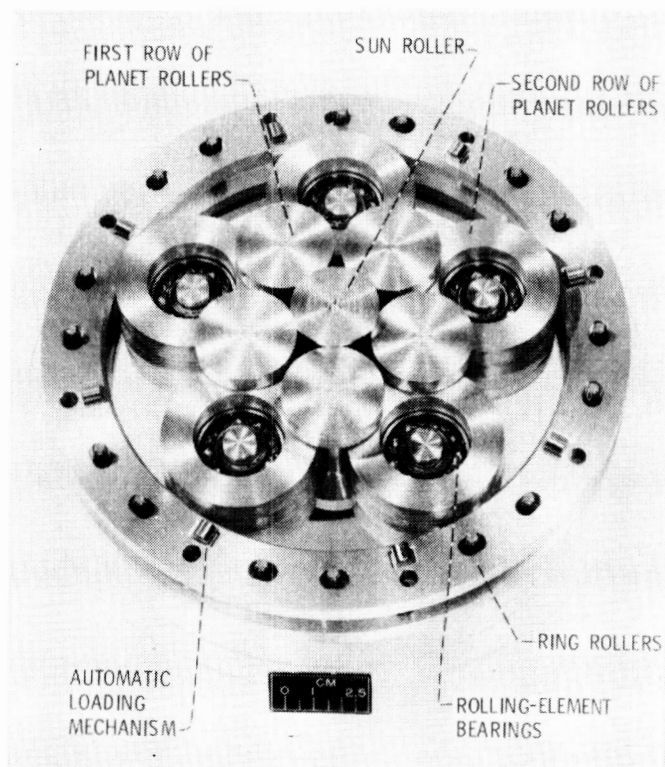


Figure 1. - Basic geometry of a Nasvytis multiroller traction drive.

with the loading mechanism contained in the ring assembly. This ring-loader drive had speed ratios between the sun and the first planet, first and second planet, and between the second planet and ring roller of 1.28, 3.87, and 2.97, respectively, for a nominal drive ratio of 14.7. The second test drive had the loading mechanism incorporated into the sun roller. The sun-loader drive had speed ratios of 1.21, 3.94, and 2.93 across these respective contacts, for a nominal drive ratio of 14.0.

Both test drives were equipped with a loading mechanism that automatically adjusted the normal contact load between the rollers in proportion to the transmitted torque. These mechanisms operated above some preselected, minimum preload setting. The automatic loading mechanism insured that there was always sufficient normal load to prevent slip under the most adverse operating conditions without needlessly overloading the contact under light loads. Thus, the load mechanism improved part load efficiency and extended drive service life.

In the case of the ring-loader drive, the loading mechanism consisted of eight small rollers contained in wedge-shaped pockets, equally spaced circumferentially between the ring rollers and the backing rings as illustrated in figures 1 and 2. The inside diameters of the ring rollers and outside diameter of the second row planets had slightly tapered (5.7°) contact surfaces. When torque was applied, the ring rollers would either circumferentially advance or retreat relative to the backing rings. This would cause the loading rollers to move up the ramped pocket, squeezing the ring rollers together axially and, in turn, radially loading the roller cluster through the tapered contact. The amount of normal force imposed on the traction-drive contacts for a given torque, or, in other words, the applied traction coefficient, could be varied by simply changing the slope of the wedge-shaped pockets. In this investigation the loading mechanism was designed to produce a constant applied traction coefficient of 0.05 for torques in excess of the initial preload values of about 25 to 40 percent of the maximum value.

The drive equipped with the sun-roller loading mechanism used the same principle, but loaded the drive radially outward through a two-piece, sun roller. Packaging the loading mechanism into the sun roller simplified the drive design and reduced the cluster weight from 9.0 kg for the ring drive down to 7.6 kg for the sun-loader design. Both test drive roller clusters were roughly of the same size, being approximately 21 cm in overall diameter and 6 cm wide.

The ring and planet rollers of both drives and the two-piece, sun roller of the sun drive were fabricated from consumable vacuum-melted (CVM) SAE-9310 (AMS-6265) steel, case carburized to a Rockwell C hardness of 60 to 62. The sun roller on the ring drive was made of through-hardened CVM, AISI 52100 steel of similar hardness. All roller running surfaces were ground to $0.2 \mu\text{m rms}$ or better.

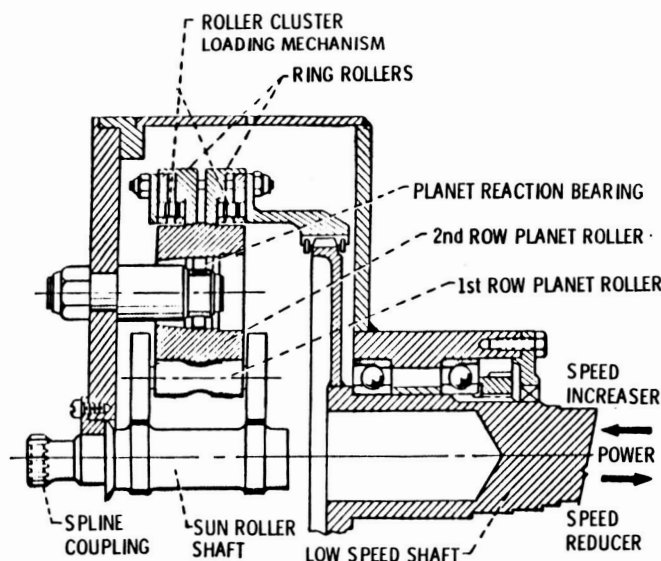


Figure 2. - Cross section of ring-loader Nasvytis traction drive.

Traction Power Transfer

In a traction drive torque is mainly transmitted by shear forces acting through a thin, elastohydrodynamic (EHD) lubricant film which separates the driving and driven rollers. Under the high pressures and severe shear rates present within a typical traction contact, the lubricant is thought to be transformed into an amorphous solid or plastic-like material (ref. 15). Because of this lubricant transformation within the EHD film, appreciable torque transfer can occur without appreciable metal-to-metal contact or wear.

The torque capacity of a given traction contact is strongly dependent on the maximum available traction coefficient, that is, the peak value of the ratio of tangential-to-normal force before gross slip. Figure 3 shows a typical traction coefficient versus creep curve for Santotrac 50, one of the two synthetic cycloaliphatic hydrocarbon traction fluids used in this investigation. The other test fluid used was Santotrac 40. These traction lubricants offer about a 50-percent improvement in traction coefficient over mineral oils and exhibit good fatigue-life performance (ref. 2). Santotrac 50 and Santotrac 40 have comparable traction coefficients, but the 50 grade is slightly more viscous and has a complete additive package. Their physical properties are reported in (ref. 2).

The curve in figure 3 was generated under the operating conditions noted with the twin-disk machine described in (ref. 16). Imposing a traction force across a lubricated disk contact, rotating at an average surface velocity U , gives rise to a differential surface velocity ΔU . The ratio of ΔU to U is generally referred to as creep in traction-drive terminology. Traction drives with a torque sensitive roller-loading mechanism generally operate at a nearly fixed value of μ . This value is selected to be sufficiently below the peak value of μ to assure safe operation. In this region creep arises from the viscoelastic and plastic straining of the plastic-like lubricant material together with the plastic, tangential deformation or compliance of the disk material. In fact for a typical steel traction-drive contact operating at high pressures (greater than 1.2 GPa) and lubricated with a traction fluid, most of the creep is observed to take place in the disks and not in the fluid film (ref. 17).

Since the creep rate represents a loss in speed, each percentage point loss due to creep represents a percentage-point loss in efficiency. Design operating conditions should be selected to maximize the available traction coefficient and minimize the creep rate. As shown in figure 3, an increase in surface speed tends to decrease μ and increase creep. An increase in contact temperature or spin as well as a decrease in contact pressure tends to do the same.

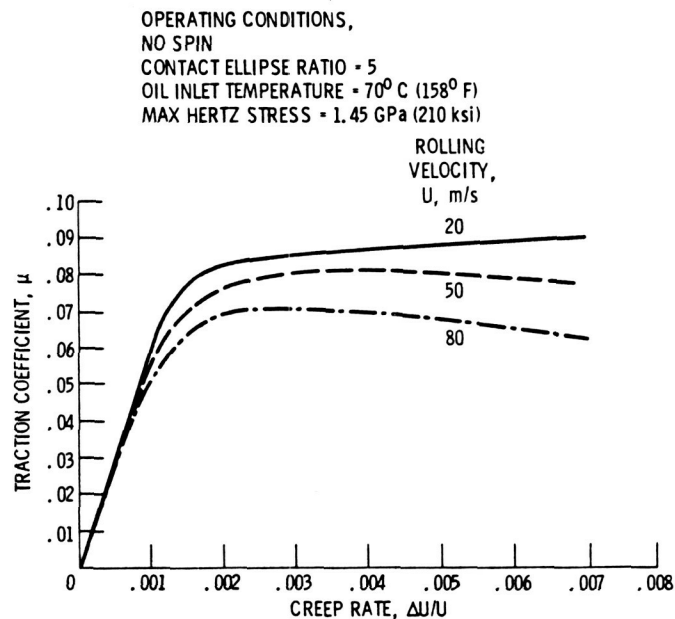


Figure 3. - Typical traction data for a traction fluid (Santotrac 50) from a twin-disk test rig described in reference 16.

Parametric Performance Tests

Apparatus

Both Nasvytis drive variants were parametrically tested on a specially constructed back-to-back test stand, described in detail in (ref. 14). In this stand, two identical drives were tested concurrently with their sun-roller shafts coupled via a flexible spline coupling. One drive functioned as the speed increaser; the other unit as the speed reducer.

Efficiency was determined by comparing, at the same operating conditions, the total test-stand power losses with the test drives in place to the test-stand tare power losses with the test drives removed. The test-stand tare power losses were measured under load by replacing the test drives with a dummy shaft. With this technique, peak efficiency can be determined accurately to within ± 0.3 percent. By measuring the flow rate, the temperature rise across the cooling oil, and the temperature of each drive housing, a heat balance method was developed, as reported in reference 14, to proportion the total power loss between each test model according to its heat dissipation. In this way differences in efficiency between the speed increaser and speed reducer test units could be estimated.

Procedure

Typically, the back-to-back increaser and reducer test drives were tested at constant input speed while the output torque on the reducer unit was increased in uniform increments until the maximum required torque level was attained. At this point the torque was dropped to the initial level, the next level of speed was set, and the process was repeated. To insure steady-state readings, typically 45 to 60 minutes of running was required between speed changes and 5 to 15 minutes between torque changes.

During these tests a nominal oil inlet temperature of 65°C was maintained at a total flow rate of 8.3 l/min. Approximately 60 percent of this oil was used to cool the sun roller with the rest going to the drive bearings and remaining drive rollers. Santotrac 40 was used as the test lubricant.

Results and Discussion

The effect of sun-roller speeds to 46 000 rpm and torques to 42 N·m on the power loss of the sun-loader variant, Nasvytis traction drive is presented in figure 4. The results from five independent test runs show that the test data are reasonably consistent. The heat balance technique mentioned previously was used to proportion the total power loss between the speed reducer and increaser. With this technique the reducer exhibited slightly higher losses than the increaser, particularly at the lower torque levels. The variation in power loss with torque is nearly linear above torque levels of about 40 percent in the region where the roller cluster loading mechanism is operating. This trend is generally in accordance with the traction-performance prediction techniques of reference 17. This analysis indicates that the contact power loss is composed of two major components, a traction creep loss term and a spin torque term, both of which are directly proportional to transmitted torque at constant creep rate.

Also apparent in figure 4 is the zero torque or tare power loss value for the test drives. The principal constituents of this tare loss are the nonslip or rolling traction contact losses of the rollers under the initial preload and miscellaneous bearing and drive-element churning and windage losses. As in the case of gears (ref. 18), these tare losses can represent a significant portion of the total drive loss, particularly at the lower torque levels and higher speeds. It is expected that lowering the initial preload levels to 5 or 10 percent of the maximum rated torque could reduce these tare power losses by up to a third, based on the data of figure 4.

The variation in increaser and reducer efficiency as a function of input torque for the sun- and ring-loader test drives is presented in figure 5. The ring-loader drives were tested to a maximum sun-roller speed and torque of 73 000 rpm and 20 N·m. The cross-hatched region represents the relatively small influence that operating speeds from 25 to 100 percent of maximum have a overall efficiency. As would be expected, the lowest speeds which produce the lowest relative tare losses and lowest creep rate resulted in the highest efficiency at a given torque level.

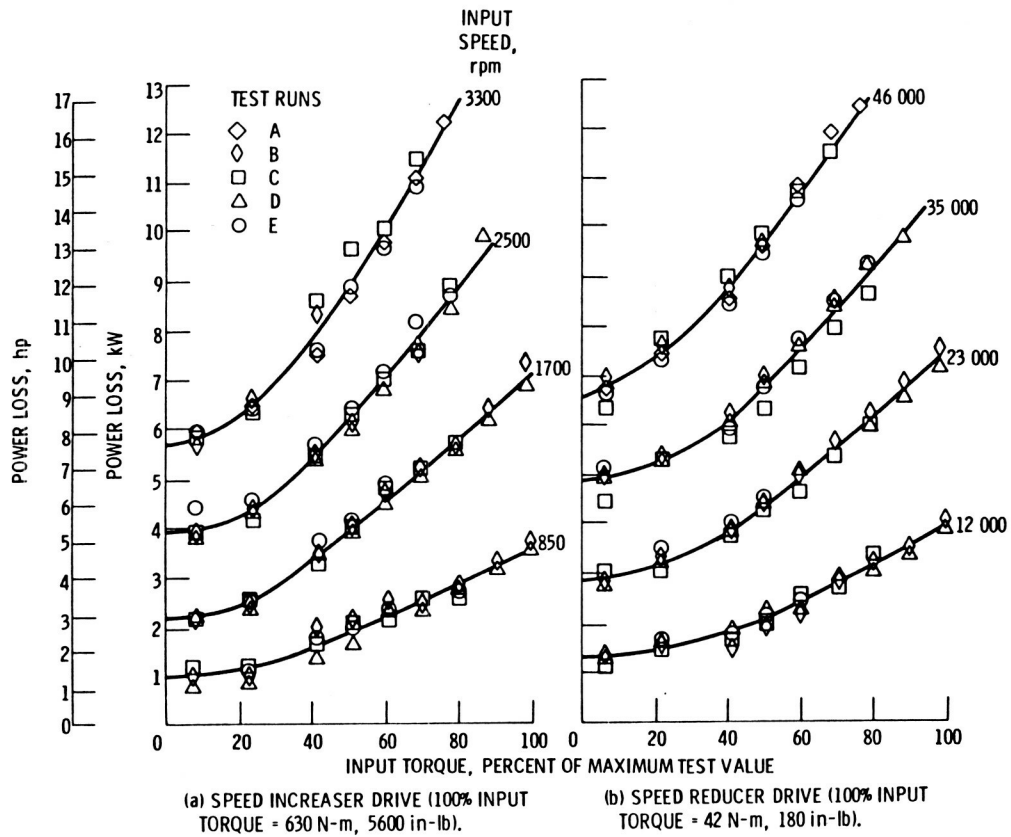


Figure 4. - Power loss of sun-loader test drive as function of input torque and speed.

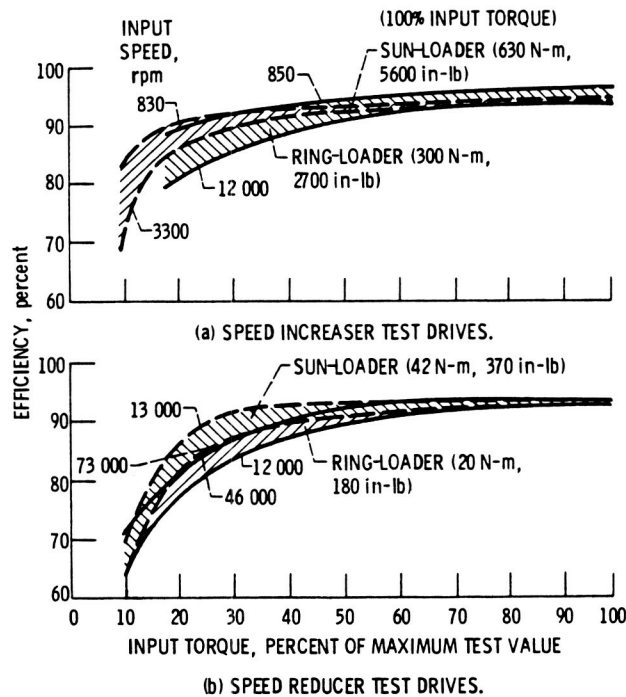


Figure 5. - Comparison of sun and ring-loader Nasvytis drive efficiencies as function of input torque and speed.

In general, the ring-loader drive had slightly higher peak efficiency values than the sun-loader unit (96 versus 94 percent for the speed increaser and 94 versus 93 percent for the speed reducer, respectively). Part of this difference is attributed to the somewhat tighter conformity of the planet and ring-roller contact surfaces in the sun-loader drive. Tighter contact conformity causes some reduction in contact stress (see fig. 6) but at the expense of slightly higher spin losses and higher creep. Although the tapered sun-roller contact in the sun-loader drive has less conformity than the sun contact in the ring unit, its tapered geometry and high roller speed contribute to higher spin losses and creep rate.

The effect of operating torque and speed on test drive creep rate is shown in figure 7. The total loss in efficiency due to creep across the drive's three contacts is generally less than about 3.5 percent for the sun-loader drives and less than 2 percent for the ring-loader units. At comparable torque levels, their creep rates were similar. Creep curves generally rise in a linear fashion with an increase in torque during the initial fixed-preload region of operation and level out as the roller-loading mechanism begins to function (see fig. 7). This behavior can be understood by examining the traction-versus-creep curves of figure 3. As the traction force is increased on a roller with a given initial normal load, the traction coefficient increases from zero, causing a corresponding linear increase in creep. At the design value of traction coefficient, the loading mechanism is activated. At this point the creep rate is held essentially constant except for small variations due to changes in the slope of the traction curve. Some degradation in creep rate performance with torque was observed for the sun-loader, reducer test model.

To determine the effectiveness of the roller-loading mechanism, a proximity probe was installed in the sun-loader drive. The probe monitored the axial position of one side of the two-piece sun-roller assembly. In this drive, as the tapered sun-roller halves moved together, the normal load on the roller-cluster was correspondingly increased. During the initial preload region of operation (fig. 8),

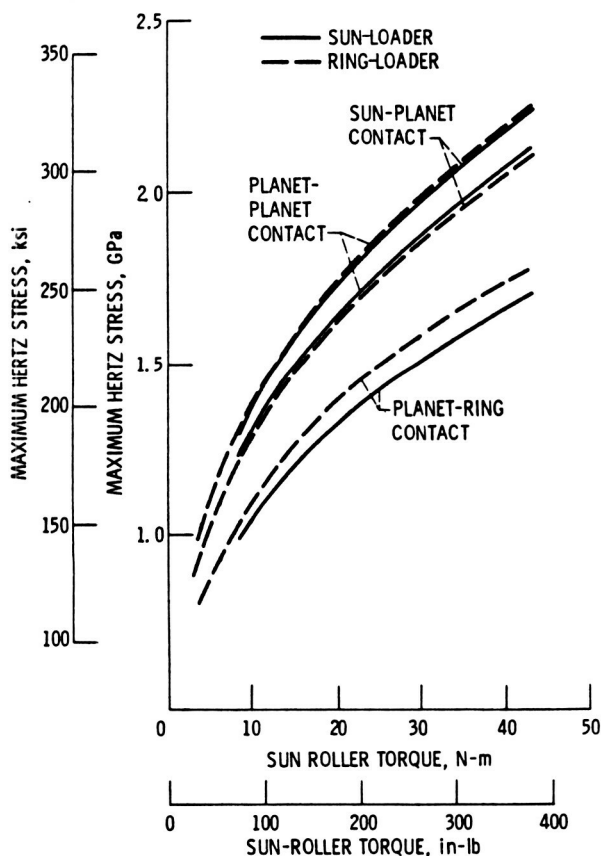


Figure 6. - Comparison of maximum Hertz stress for sun- and ring-loader drive contacts.

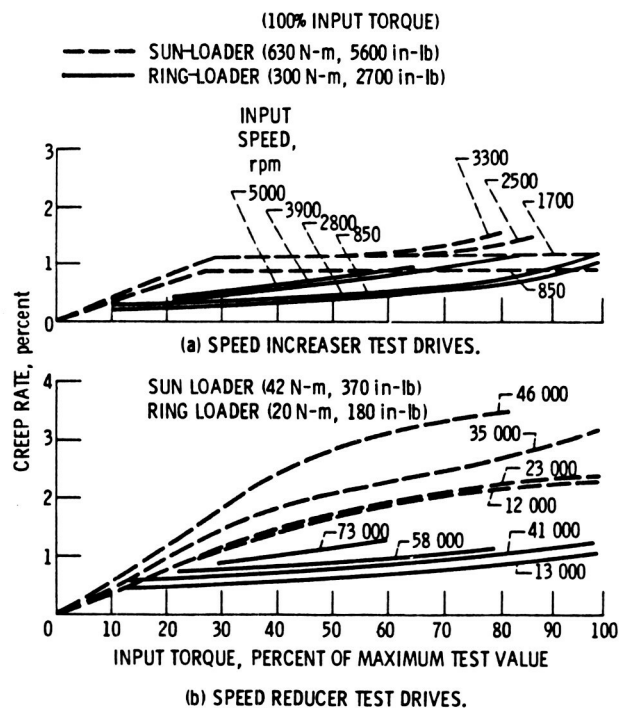


Figure 7. - Comparison of sun- and ring-loader Nasvytis drive creep rates as a function of input torque and speed.

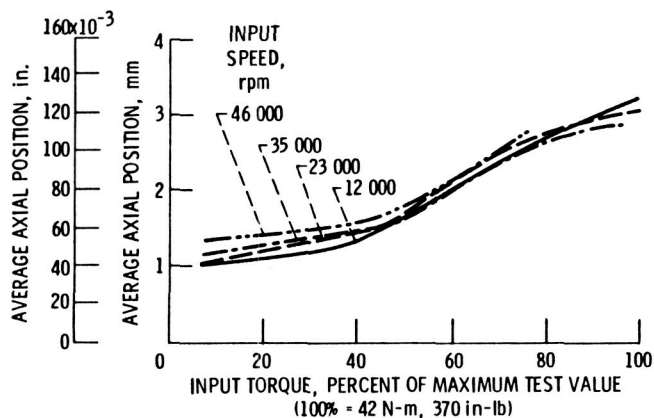


Figure 8. - Average axial position of loading mechanism in sun-loader Nasvytis drive.

the sun-roller position was reasonably constant up to a torque level of approximately 40 percent. Above 40 percent, the sun-roller halves move inward together in a nearly linear fashion with increasing torque, indicating satisfactory roller-loading action. Because of a centrifugal force effect on the loading balls, an increase in speed causes a slight increase in initial preload. The loading mechanisms on both the speed increaser and reducer test units showed similar behavior.

Temperatures of the rollers in the test drives increased steadily with an increase in operating speed. The sun-roller temperature, as measured by a thermocouple near the surface, was higher than any other component in the drive. Sun-roller temperatures never exceeded approximately 110° and 150° C for the sun- and ring-loader drives, respectively.

Gas Turbine Engine Tests

Parametric dynamometer tests were conducted with a Nasvytis traction drive that had been incorporated into 112 kW (150 hp) automotive gas-turbine engine. For this installation, the 14-to-1 ratio roller cluster from the sun-loader test drive was retrofitted into the engine's power turbine assembly in place of the original 9.7 to 1 helical gear mesh. A cross section of the Nasvytis drive installation within the power-turbine housing is shown in figure 9. The sun roller was coupled to the end of the power turbine rotor through a semiflex spline coupling. The ring roller was spline coupled to the output shaft, which, in turn, would normally drive the vehicle's automatic transmission. However, for this test, the output shaft of the drive was directly coupled to a power absorbing dynamometer via a prop shaft.

Modifications to the original power-turbine assembly included the replacement of the rotor's rear fluid-film journal bearing and hydrostatic thrust bearing with a thrust carrying, split-inner-race, angular-contact ball bearing. Changes were made to the power-turbine housing to incorporate the concentric Nasvytis drive. The self-supported sun roller eliminated the need for the high-speed, fluid-film bearings, which normally straddle the pinion and react gear-tooth separating loads.

Two series of parametric tests were conducted on the traction-drive-equipped turbine engine under nominally the same test conditions as described earlier for the back-to-back stand tests. However, power-turbine speeds were limited to 45 000 rpm and power levels to 112 kW. Santotrac 50 was used as the test oil. In the first series of tests the sun-roller loading mechanism was locked out, and a fixed preload was set at the value required to prevent gross slip under full load. The second series of tests made use of the variable, sun-roller loading mechanism.

Figure 10 shows the comparative efficiency results from these two test series. The efficiency values shown in this figure were estimated from the increase in heat content of the cooling oil as it passed through the drive cavity. Using a similar heat balance estimate, an efficiency value was assigned to the rotor's front fluid-film journal bearing and rear ball bearing based on the heat power dissipated to the bearings' cooling oil. Although this heat balance method is rather imprecise, due to the uncertainties in the amount of heat either dissipated by the cooling oil to the power-turbine housing or vice versa, the efficiencies from the back-to-back stand measurements and those estimated by this method (fig. 10) are similar.

The data in figure 10 show that the equivalent efficiency of the power-turbine rotor bearings as well as the efficiency of the Nasvytis drive are relatively speed insensitive. It is also apparent from figure 10 that the fixed-preload operation causes an appreciable decrease in part-load efficiency. At the high torque levels, the variable loading mechanism imposes a normal load approaching that of the fixed-preload system, and their respective efficiencies merge as would be expected.

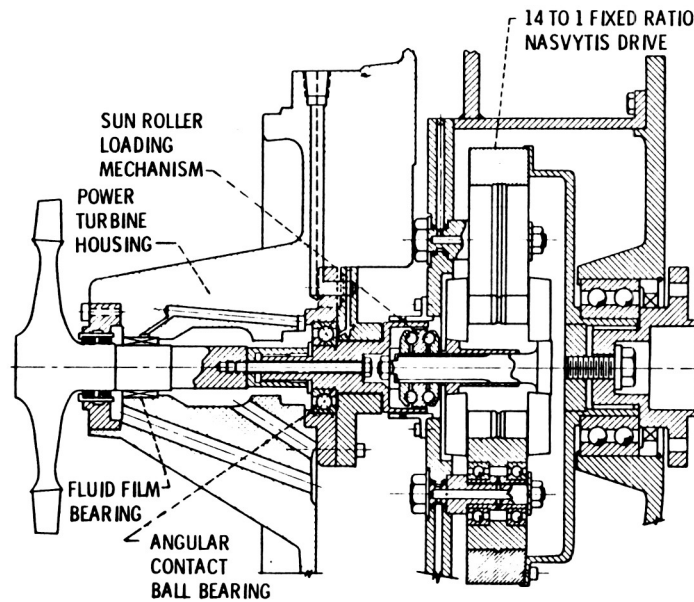


Figure 9. - Installation of Nasvytis traction drive with power turbine assembly.

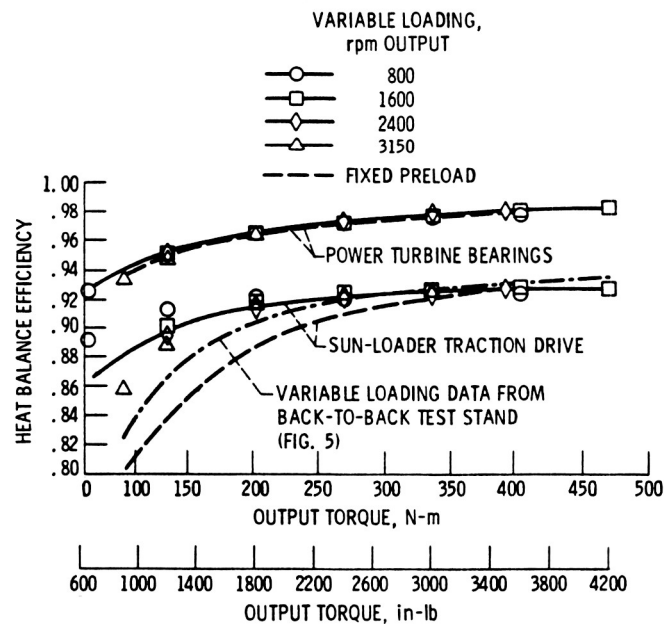


Figure 10. - Heat balance efficiency of sun-loader Nasvytis drive from gas-turbine-engine tests as compared with back-to-back test stand measurements.

Creep rate data for the engine tests are presented in figure 11. Also included for comparison are the back-to-back stand data from figure 7 for the sun-loader reducer drive at 35 000 rpm. The agreement between both sets of creep data is within 0.2 percentage point at all corresponding test speeds (not shown in fig. 7) except at 44 000 rpm. At this speed the stand measurements indicate about 0.5 percentage point greater creep rate than the engine test data at the higher torque levels.

Although the creep rate associated with fixed-preload operation is about 0.6 percentage point less than that with variable preloading (fig. 11), the overall efficiency is decidedly inferior (fig. 10) because of contact overloading. The lower creep rate is due to the high initial normal load associated with fixed preload operation. This lowers the applied traction coefficient so that the resulting creep rate from the traction curve (see fig. 3) will also be relatively small. Also the upward trend of the fixed-preload creep data suggests that a slip condition is being approached.

In general, the Nasvytis drive demonstrated good operational compatibility and performance with the gas-turbine engine throughout the engine's torque and speed range. Orthogonal, radial proximity probes mounted at two axial positions along the power-turbine shaft, showed that the coupled rotor-traction-drive system was reasonably stable from engine idle to maximum speed. No synchronous whirl instabilities were encountered. Temperature distributions of rollers and bearings were quite satisfactory, similar to those obtained in the back-to-back stand tests.

Capacity and Durability

Traction drives, like rolling-element bearings, are generally sized on the basis of rolling-element fatigue life. This is because, for most applications other than those that are particularly short lived, the stress levels required for acceptable fatigue life are generally well below those for static yield failure. For example, maximum bending stresses in the Nasvytis test drives at a peak sun-roller torque of 42 N·m is less than 350 MPa, and maximum contact stresses are less than 2.2 GPa. For the case-hardened steel rollers in the Nasvytis drive, the expected yield stress in bending would be approximately 1400 MPa and the Brinelling stress limit would be on the order of 4 GPa.

Because of these relatively low maximum operating stress levels, occasional momentary overloads, several times the maximum design value can generally be tolerated. Furthermore, if these transient overloads are of a brief duration and do not occur too frequently, then only a relatively small penalty to the drives' total fatigue life will result.

A traction drive's sensitivity to shock loads is also dependent on the ability of the contact surface to avoid skidding or heating damage. If the drive is equipped with a fast acting loading mechanism,

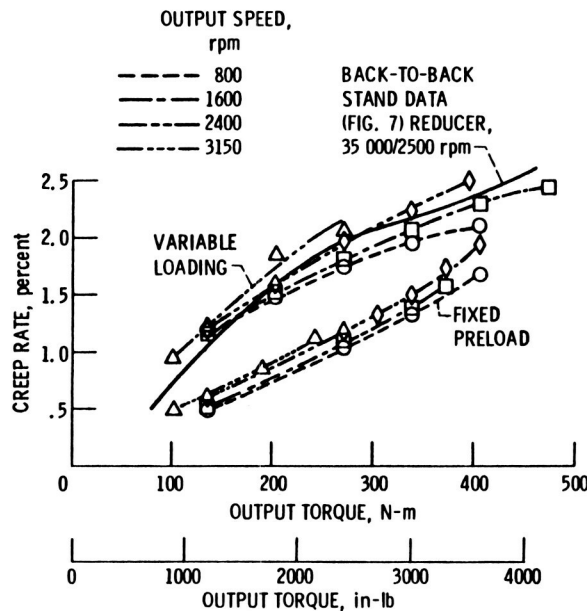


Figure 11. - Comparison of fixed preload and variable loading creep rate for sun-loader reducer from gas-turbine-engine tests. Drive ratio, 14.

such as the mechanical type used in the Nasvytis test units, and if the overload is of sufficiently short duration to avoid overheating the contact, then no surface damage would be expected.

The normally expected failure mode of a properly-designed traction drive will be rolling-element fatigue. This failure criterion is exactly analogous to pitting failure in gears and spalling failure in rolling-element bearings. The risk of wear or scuffing failures of traction-drive contacts can be eliminated or greatly minimized through the use of proper materials and also proper lubricating and cooling design practices such as those that have been successfully applied in bearing and gear design. In view of this similarity in the failure mechanism, it is anticipated that the fatigue-life theory of Lundberg and Palmgren (ref. 19), the accepted method of establishing load capacity ratings for rolling-element bearings by bearing manufacturers, can be adapted to predict traction-drive service life. In reference 7 the basic life equations for traction drives were developed from Lundberg-Palmgren theory and applied to a toroidal traction drive. Life adjustment factors due to advances in materials, lubricants, and design technology were also considered. In reference 20 this life analysis was applied to the Nasvytis traction-drive geometry. Theoretical B_{10} (90-percent survival) life ratings for the Nasvytis test drives based on the work of reference 20 appear in figure 12. These data were generated at a constant sun-roller speed of 50 000 rpm. It includes a life-adjustment factor of 6 for through-hardened CVM AISI-52100 or case-hardened CVM AMS-9310 steels, a life factor of approximately 2.5 for a favorable film thickness-to-surface roughness ratio, and an estimated life penalty of 0.5 for the potentially adverse effects of traction on fatigue life.

At a given required life level (fig. 12), the sun-loader test unit shows slightly higher power capacity than the ring-loader traction drive. Continuous power capacity ranged from 42 kW for 10 000 hours of system life to 185 kW for a minimum of 100 hours at sun-roller speeds of 50 000 rpm (or about 3500 rpm on the low-speed shaft). Increasing the size of the drive has a significant increase in power capacity. Reference 7 reports that traction drive fatigue life, L , is related to size factor and to torque T as follows:

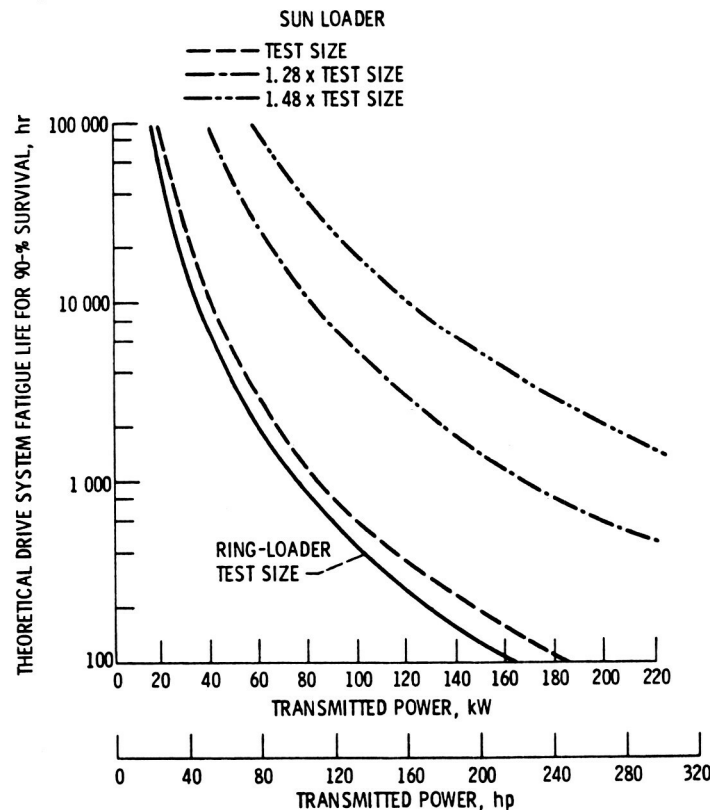


Figure 12. - Effect of size and power on theoretical Nasvytis drive fatigue life at a sun-roller speed of 50 000 rpm.

$$L \propto (\text{size factor})^{8.4}$$

and

$$L \propto T^{-3}$$

It, therefore, follows that the torque capacity of the drive for a given required fatigue life is related to size by

$$T \propto (\text{size factor})^{2.8}$$

Thus, increasing the test drive size by 28 percent, that is, increasing the roller-cluster's overall diameter to 27 cm and width to 8 cm, will double torque capacity at a given life level. Similarly a 48-percent size increase will more than triple the load capacity, as illustrated in figure 12. This scaling assumes that the design or applied traction coefficient remains constant with size. However, with an increase in size, the rolling surface speed of the contact increases and the contact stress decreases, causing some loss in the available peak traction coefficient. If additional roller-loading is needed to compensate for this loss in traction coefficient, then a small life derating will be needed.

The capacity ratings shown in figure 12 are for the test drive geometry under the specified operating conditions. These ratings can change significantly with changes in drive geometry. The most durable traction-drive geometry (the number of planet rows, the number of planet rollers in each row, and the relative diameter ratios at each contact) can be determined for a given application from a computerized optimization technique such as that described in (ref. 21).

Summary and Conclusions

Parametric back-to-back stand tests and gas-turbine engine dynamometer tests were conducted on two fixed-ratio Nasvytis multiroller traction drives. The effects of speed and torque on drive efficiency, creep rates, temperature distribution, roller stability, and loading mechanism action were investigated. Two traction fluids were used. The 14.7 to 1 ratio ring-loader drive in which the loading mechanism was incorporated into the ring assembly, was tested to sun speeds of 73 000 rpm and power levels to 130 kW. The sun-loader drive of 14.0 to 1 ratio was tested to 46 000 rpm and 180 kW. The cluster from this drive was retrofitted to the power turbine of an automotive gas turbine in place of the original helical gear reducer. Tests were conducted to full-engine speed (45 000 rpm) and power (110 kW). The effects on drive performance of fixed-preload (constant normal load) operation were compared with those obtained with variable-roller-cluster loading (proportional to the transmitted torque). Comparisons were also made of the data from engine dynamometer tests and those obtained from the back-to-back stand tests. The sun- and ring-loader roller-clusters measured approximately 21 cm in diameter and weighed 7.6 and 9.0 kg, respectively. Predictions of test drive system fatigue life as function of size and transmitted power were made using Lundberg-Palmgren fatigue theory. Based on the above, the following results were obtained:

1. The ring- and sun-loader test drives exhibited peak efficiency levels of 96 to 94 percent, respectively, for the speed increaser units and 94 and 93 percent, respectively, for the speed reducer units.
2. The Nasvytis drive showed good operational compatibility with the gas-turbine engine. Test data from these engine tests showed reasonable agreement with the back-to-back stand tests.
3. Efficiency loss due to creep was generally less than 3.5 percent for the three drive contacts under the worst-test conditions.
4. Theoretical fatigue lives of the sun- and ring-loader drives were comparable. The 90-percent survival life rating ranged from 10 000 hours at 42 kW to 100 hours at 185 kW for a sun-roller speed of 50 000 rpm. A 28-percent increase in size would theoretically double these power ratings.

References

1. Carson, R. W.: Traction Drives Update, *Power Transmis. Des.*, vol. 19, no. 11, Nov. 1977, pp. 37-42.
2. Loewenthal, S. H.; and Parker, R. J.: Rolling-Element Fatigue Life with Two Synthetic Cycloaliphatic Traction Fluids. NASA TN D-8124, 1976.
3. Magi, M.: On Efficiencies of Mechanical Coplanar Shaft Power Transmissions. Chalmers University, Gothenburg, Sweden, 1974.
4. Gaggermeier, H.: Investigations of Tractive Force Transmission in Variable Traction Drives in the Area of Elastohydrodynamic Lubrication. Ph. D. Dissertation, Technical University of Munich, July 1977.
5. Tevaarwerk, J. L.; and Johnson, K. L.: The Influence of Fluid Rheology in the Performance of Traction Drives. *J. Lubr. Technol.*, vol. 101, no. 3, July 1979, pp. 266-274
6. Daniels, B. K.: Non-Newtonian Thermo-Viscoelastic EHD Traction from Combined Slip and Spin. *ASLE Preprint* 78-LC-2A-2, Oct. 78.
7. Coy, J. J.; Loewenthal, S. H.; and Zaretsky, E. V.: Fatigue Life Analysis for Traction Drives with Application to a Torodial Type Geometry. NASA TN D-8362, 1976.
8. Rohn, D. A.; Loewenthal, S. H.; and Coy, J. J.: Simplified Fatigue Life Analysis for Traction Drive Contacts. *J. Mech. Des.*, vol. 103, no. 2, Apr. 1981, pp. 430-438, discussion, pp. 438-439.
9. Hewko, L. O.; Rounds, F. G., Jr.; and Scott, R. L.: Tractive Capacity and Efficiency of Rolling Contacts. *Rolling Contact Phenomena*, J.B. Bidwell, ed., Elsevier Publ. Co., Amsterdam, 1962, pp. 157-185.
10. Hewko, L. O.: Contact Traction and Creep of Lubricated Cylindrical Rolling Elements at Very High Surface Speeds. *ASLE Trans.*, vol. 12, no. 2, Apr. 1969, pp. 151-161.
11. Hewko, L. O.: Roller Traction Drive Unit for Extremely Quiet Power Transmission. *J. Hydronaut.*, vol. 2, no. 3, July 1968, pp. 160-167.
12. Nakamura, L.; et al.: A Development of a Traction Roller System for a Gas Turbine Driven APU. SAE Paper No. 790106, Feb. 1979.
13. Nasvytis, A. L.: Multiroller Planetary Friction Drives. SAE Paper No. 660763, Oct. 1966.
14. Loewenthal, S. H.; Anderson, N. E.; and Nasvytis, A. L.: Performance of a Nasvytis Multiroller Traction Drive. NASA TP-1378, 1978.
15. Smith, F. W.: The Effect of Temperature in Concentrated Contact Lubrication. *ASLE Trans.*, vol. 5, no. 1, Apr., 1962, pp. 142-148.
16. Johnson, K. L.; and Tevaarwerk, J. L.: The Shear Behaviour of Elastohydrodynamic Oil Films. *Proc. Roy. Soc. (London)*, ser. A, vol 356, no. 1685, Aug., 1977, pp. 215-236.
17. Tevaarwerk J. L.: Traction Drive Performance Prediction for the Johnson and Tevaarwerk Traction Model. NASA TP-1530, 1979.
18. Anderson, N. E.; and Loewenthal, S. H.: Part and Full Load Spur Gear Efficiency. NASA TP-1979.
19. Lundberg, G.; and Palmgren, A.: Dynamic Capacity of Rolling Bearings. *Ingeniorsvetenskapsakademiens, Handlinger*, No. 196, 1947.
20. Coy, J. J.; Rohn, D. A.; and Loewenthal, S. J.: Life Analysis of a Nasvytis Multiroller Traction Drive. NASA TP-1980.
21. Coy, J. J.; Rohn, D. H.; and Loewenthal, S. H.: Constrained Fatigue Life Optimization of a Nasvytis Multiroller Traction Drive. *J. Mech. Des.*, vol. 103, no. 2, Apr. 1981, pp. 423-428, discussion pp. 428-429.